

E. SKOLEK*, K. DUDZIŃSKA*, J. KAMIŃSKI*, W.A. ŚWIĄTNICKI*

CORROSION RESISTANCE OF THE BEARING STEEL 67SiMnCr6-6-4 WITH NANOBAINITIC STRUCTURE

ODPORNOŚĆ KOROZYJNA STALI ŁOŻYSKOWEJ 67SiMnCr6-6-4 O STRUKTURZE NANOKRYSTALICZNEJ

The paper describes a comparative study of the corrosion resistance of bearing steel 67SiMnCr6-6-4 after two kinds of nanostructuring treatments and two kinds of conventional quenching and tempering treatments. The nanostructuring treatment consisted of austempering with an isothermal quenching at 240°C and 300°C. The conventional heat treatment consisted on quenching and tempering at 350°C for 1 h and quenching and tempering at 550°C for 1 h. Time and temperature of tempering was chosen so that the hardness of both samples (nanostructured as well as quenched and tempered) was similar. The microstructure of steel after each heat treatment was described with the use of transmission electron microscopy (TEM). It was shown, that the austempering conducted at 240°C produced homogenous nanobainitic structure consisting of carbide-free bainite plates with nanometric thickness separated by the layers of retained austenite. The austempering at 300°C produced a sub-micrometric carbide-free bainite with retained austenite in form of layers and small blocks. The conventional heat treatments led to a tempered martensite microstructure. The corrosion resistance study was carried out in Na₂SO₄ acidic and neutral environment using potentiodynamic and electrochemical impedance spectroscopy (EIS) methods. The corrosion resistance of nanostructured steel samples were compared to the steel samples with tempered martensite. The obtained results indicate, that the corrosion resistance of bearing steel with nanobainitic structure is similar to steel with tempered martensite in both acidic and neutral environment. This means that the high density of intercrystalline boundaries in nanobainite does not deteriorate the corrosion properties of the bearing steel.

Keywords: bearing steel, austempering, nanocrystalline structure, corrosion resistance, nanobainite

W pracy przedstawiono porównawcze badania odporności korozyjnej łożyskowej stali 67SiMnCr6-6-4 poddanej dwóm typom procesów nanostrukturyzacji oraz dwóm typom konwencjonalnych obróbek hartowania i odpuszczania. Obróbka nanostrukturyzacji polegała na hartowaniu z przystankiem izotermicznym w temperaturze 240°C oraz 300°C. Konwencjonalna obróbka cieplna obejmowała hartowanie i odpuszczanie w temperaturze 350°C przez 1 h oraz hartowanie i odpuszczanie w temperaturze 550°C przez 1 h. Czas i temperatura odpuszczania dobrane były tak, aby twardość próbek (po nanostrukturyzacji oraz hartowaniu i odpuszczaniu) była zbliżona. Mikrostruktura stali po różnych obróbkach cieplnych określona była przy użyciu transmisyjnego mikroskopu elektronowego. Wykazano, że hartowanie izotermiczne w temperaturze 240°C pozwoliło na wytworzenie jednorodnej struktury nanobainitycznej, zbudowanej z płytek bezwęglkowego bainitu, porozielenych warstwami austenitu szczątkowego. Podczas hartowania izotermicznego w temperaturze 300°C wytworzono bainit bezwęglkowy o submikronowej wielkości ziaren z austenitem szczątkowym w postaci warstw oraz niewielkich bloków. W wyniku konwencjonalnych obróbek hartowania i odpuszczania wytworzono martenzyt odpuszczony. Badania odporności korozyjnej przeprowadzono metodą elektrochemicznej spektroskopii impedancyjnej (EIS) oraz metodą potencjo dynamiczną, w kwaśnym oraz obojętnym środowisku Na₂SO₄. Odporność korozyjną stali po obróbkach nanostrukturyzacji porównano z odpornością korozyjną stali o strukturze martenzytu odpuszczonego. Otrzymane wyniki wskazują że zarówno w środowisku kwaśnym jak i obojętnym odporność korozyjna stali łożyskowej o strukturze nanokrystalicznej jest zbliżona do odporności korozyjnej tej stali o strukturze martenzytu odpuszczonego. Oznacza to, że duża gęstość granic ziaren w strukturze nanobainitu nie pogarsza odporności korozyjnej stali łożyskowej.

1. Introduction

One of the most promising directions of materials development is formation inside of them a nanocrystalline structure, in which the grains size, in at least one direction is lower than 100 nm [1]. The nanocrystalline structure improves the properties of materials and thus, it allows extending the scope of their applications. The works on nanostructuring

of steel, which is the most commonly applied metallic structural material are developing very intensively. Nanocrystalline structure can be produced by various methods and the most promising method for nanostructuring of steels is based on phase transformations occurring during heat treatment [2-6]. Properly designed heat treatment allows creating a nanocrystalline structure in finished components of different shapes and cross-sections [7,8,9].

* WARSAW UNIVERSITY OF TECHNOLOGY, FACULTY OF MATERIALS SCIENCE AND ENGINEERING, 141 WOŁOSKA STR., 02-507 WARSAW, POLAND

In many cases, usable properties of presently applied steels with conventional structure are not satisfying. While using in such applications as: mining equipment, agricultural machinery, automobile parts, tracked vehicles, excavators, building equipment, armours etc., the material shall have high strength and toughness, wear resistance and corrosion resistance. The solution to such high requirements may be steels with a structure of nanocrystalline bainite. It has been shown, that such a structure can be obtained in steels at industrial scale by use of austempering heat treatment [2-9].

There are relatively few works devoted to the studies on corrosion resistance of ferrous ultrafine-grained steels [10, 11], however, the susceptibility of nanocrystalline bainite for corrosion resistance has not been clearly defined so far. The corrosion resistance depends on both: the kind of chemical and phase composition of the material as well as the corrosion environment and the corrosion type which affects the material [10-20]. That is why, the authors took an attempt to study the corrosion resistance in the acidic and neutral corrosion environment of the steel 67SiMnCr6-6-4 with a various microstructures obtained through two kinds of isothermal annealing at a temperature in the range of bainitic transformation, in comparison to the conventional quenching and tempering heat treatments applied for this steel. The parameters of quenching and tempering applied for steel samples have been chosen in order to obtain a similar hardness as in samples subjected to isothermal annealing treatments.

2. Experimental methods

67SiMnCr6-6-4 bearing steel of composition presented in Table 1 was subjected to nanostructuring treatment consisting of austempering with an isothermal quenching at 240°C for 61 h (A1) and at 300°C for 6.5 h (A2). In order to determine austempering parameters, the studies of characteristic parameters and kinetics of phase transformations in steel were carried out using the quenching dilatometer Bähr DIL 805L. The heat treatment parameters were chosen so that the temperature of austempering was above the martensite start (M_s) temperature. The duration of the austempering was established in order to complete the bainitic transformation at this temperature. A cooling medium in which the treatment was carried out was liquid Sn-Ag alloy heated to a temperature of austempering. Microstructure of the samples after heat treatments was observed using light microscope (LM), scanning electron microscope (SEM) and transmission electron microscope (TEM) operating at 120 kV. The hardness measurements were performed using Vickers diamond testing machine with an applied load of 2kG.

The corrosion resistance was examined by the potentiodynamic and Electrochemical Impedance Spectroscopy (EIS) methods in an acidic (pH4) and neutral (pH7) aerated aqueous 0.1 M Na_2SO_4 solution. Changes in pH of the solution were made with the use of sulfuric acid. Due to the high conductivity of the electrolyte (salt solution of a strong alkali and strong acid) time of 60 minutes is sufficient to form and stabilize the double layer on the boundary of the metal and electrolyte and a stable corrosion potential. The impedance measurements were performed at a corrosion potential with the frequency ranging from 10^{-3} Hz to 10^4 Hz. The amplitude of the pulse the alternating current (sinusoidal) was 20 mV. The spectra obtained were analyzed using the 3.0 Boukamp computer program. Equivalent circuit with two time constants $R(RQ)(RQ)$ was used. The results are presented in the form of the Bode diagrams, showing the relationship between $\log -Z$ (where Z is a vector length on complex plane corresponding to the impedance) or an angle θ (formed by the vector "z" of the real axis) as a function of the logarithm of frequency F . Potentiodynamic study was carried out directly after the completion of EIS study. In the potentiodynamic method the samples were polarized towards the anode from the potential 200-250 mV lower than the corrosion potential to the potential of -200 mV. The potential variation rate was 0.3 mV/s. Prior to the measurements, the samples were immersed in solution at a room temperature for 1 h to let the corrosion potential to stabilize. After examinations of the corrosion resistance, the surfaces were observed in a Hitachi S-3500N scanning electron microscope. The corrosion resistance study of bearing steel 67SiMnCr6-6-4 after nanostructuring treatment was carried out with compare to the steels after a quenching and tempering on a similar hardness – at 350°C for 1 h (QT1) and 550°C for 1 h (QT2) respectively.

3. Results

3.1. Microstructure characterisation

The observation through LM indicated, that steel after austempering treatment has a fine-grained microstructure, with a needle-shaped character, in which needles are partially located parallel towards each other and partially towards various angles creating packets and groupings distributed in various directions (Figs. 1, 2). In the observed microstructure, there are areas including large blocks of bright, not etching phase – probably austenite. The size of blocks and their total area are greater for higher temperature of the isothermal annealing.

TABLE 1

Chemical composition of 67SiMnCr6-6-4 bearing steel

	C [%]	Si [%]	Mn [%]	Cr [%]	Mo [%]	Ni [%]	P [%]	S [%]
67SiMnCr6-6-4	0.65÷0.7	1.45÷1.6	1.35÷1.55	1.00÷1.2	0.23÷0.27	max 0.25	max 0.025	0.015÷0.02

Identification and analysis of phases by means of an TEM revealed that in steel treated at 240°C, a carbide-free nanobainitic structure was formed with average width of bainitic ferrite (α_B) plates amounting to 49 ± 3.7 nm. The midribs occurred in the ferrite plates. Between the ferrite plates, there were the layers of retained austenite (γ_R) with average thickness of 39 ± 2.6 nm. The total volume fraction of residual austenite estimated on the basis of TEM micrographs amounted to ca. 38%. This microstructure was very homogeneous in the entire observed area.

After austempering at 300°C the nanometric carbide-free bainite was still present, however the structure is coarser than in case of the treatment at the temperature of 240°C. In this case, the average thickness of ferrite plates amounts to 101 ± 4.6 nm and the midribs occurred less frequently. The retained austenite appeared both in form of thin layers with an average thickness of 36 ± 1.5 nm (Fig. 6) and large blocks with average cross section area up to $2,79 \mu\text{m}^2$. The austenite blocks contained numerous dislocations and stacking faults. The overall volume fraction of residual austenite was estimated to 53%.

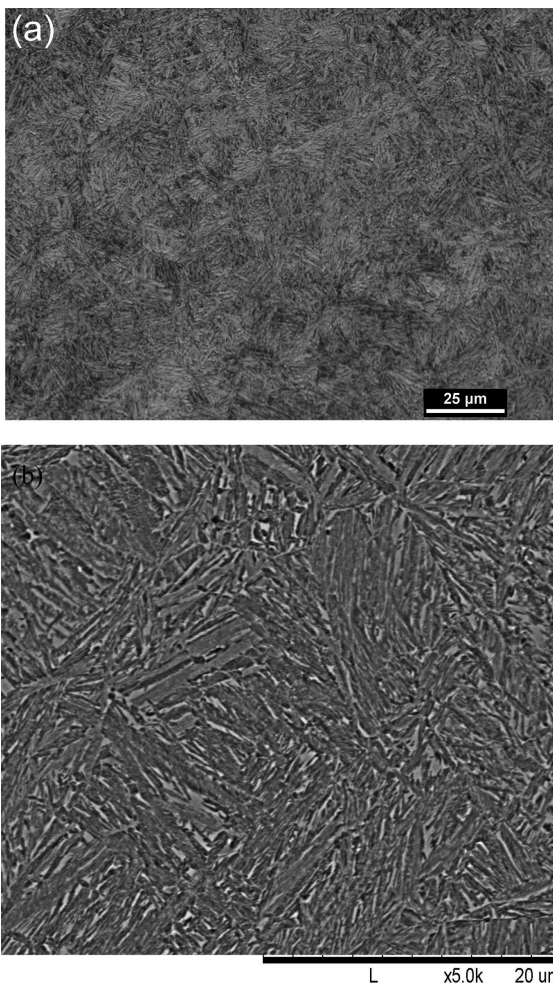


Fig. 1. Microstructure of 67SiMnCr6-6-4 bearing steel after austempering treatment at 240°C for 61h observed using light microscope (a) and scanning electron microscope (b)

Exemplary LM microstructures of the bearing steel after both nanostructuring processes at 240°C and 300°C are pre-

sented on Fig. 1 and 2 respectively. The TEM images of these microstructures are presented on Fig. 3 and 4.

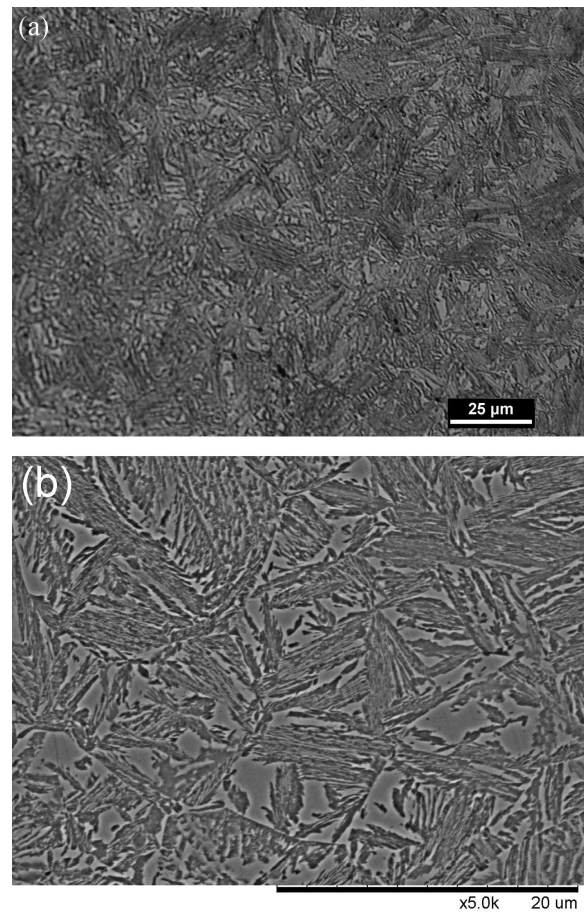
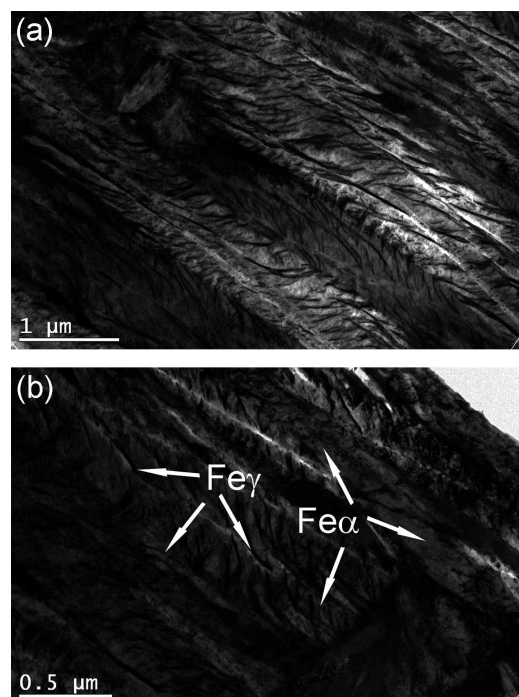


Fig. 2. Microstructure of 67SiMnCr6-6-4 bearing steel after austempering treatment at 300°C for 6.5h observed using light microscope (a) and scanning electron microscope (b)



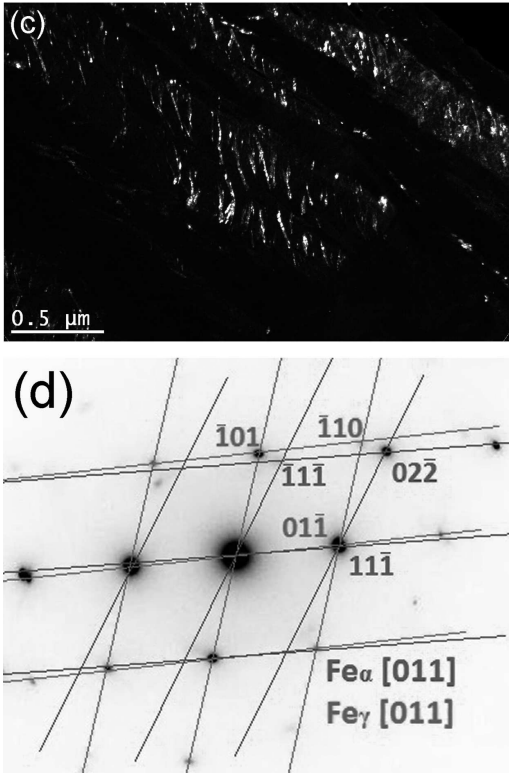


Fig. 3. Microstructure of 67SiMnCr6-6-4 bearing steel after austempering treatment at 240°C for 6h observed using transmission electron microscope: (a), (b) – bright field image, (c) – dark field image of (b) area for austenite reflection; d) diffraction pattern of (b) area

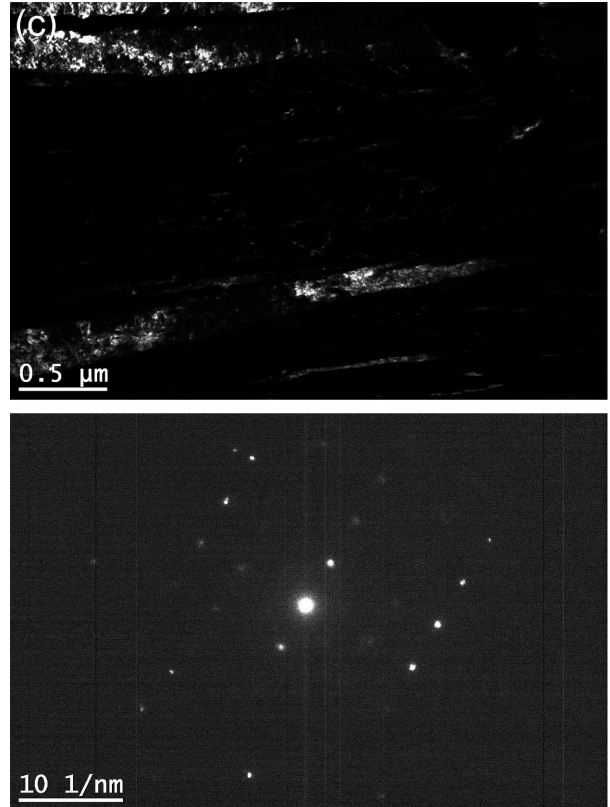
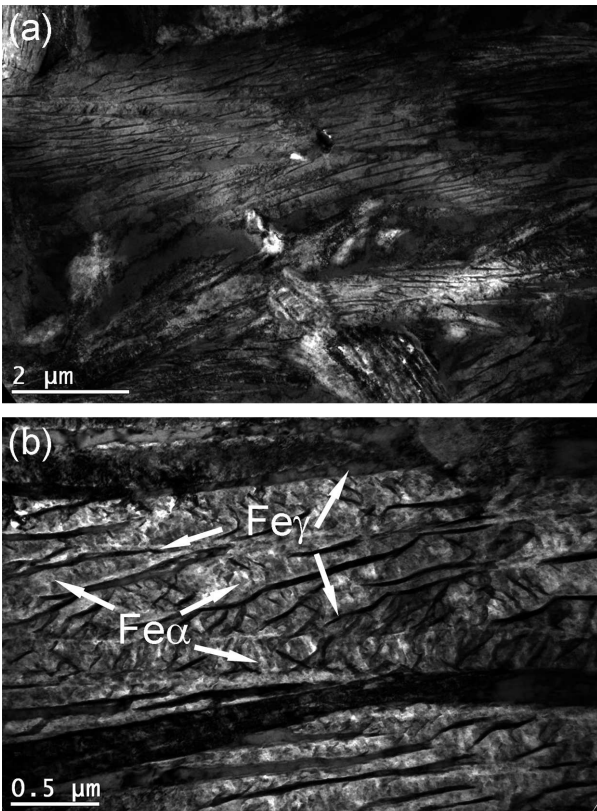


Fig. 4. Microstructure of 67SiMnCr6-6-4 bearing steel after austempering treatment at 300°C for 6.5 h observed using transmission electron microscope: (a) – blocks of retained austenite, (b) – bright field image, (c) – dark field image of (b) area for austenite reflection; d) diffraction pattern of (b) area



3.2. 3.2 Hardness measurements

The results of the hardness measurements are presented in the Table 2. Austempering treatment at low temperature leads to a hardness comparable to the hardness of steel with a nanobainitic structure that are described in the literature [21]. Increasing the temperature of the isothermal stop to 300°C, due to the increase in retained austenite content and the presence of retained austenite in the form of blocks leads to a reduction in hardness.

TABLE 2
Hardness values of 67SiMnCr 6-6-4 bearing steel after various heat treatments

treatment	A1	A2	QT1	QT2
HV2	658	514	662	495

3.3. Corrosion resistance

The study of corrosion resistance by electrochemical impedance spectroscopy indicates a similar electrochemical behavior of the steel after nanostructuring treatment and after quenching and tempering treatment (Fig. 5, Table 3). In acidic environment for both types of treatments, double, overlapping peaks of the phase angle in the impedance spectra were observed, which indicates the presence of two phases with

different corrosion resistance. Electrochemical reactions are processes of oxidation of iron Fe^0 to Fe^{+2} that occur with a varying intensity. In this environment, irrespective of tested material, first of the processes (column 3 in Table 3) is characterized by a slightly less resistance and an order of magnitude greater capacity compared to the second occurring process (column 4 in Table 3). It can be assumed that the phase with the parameter $n = 1$ does not corrode in this environment.

In a neutral environment the corrosion resistance of the steel components is similar, therefore a single dominant capacitive peak was observed. Electrochemical reaction, as in the case of an acid environment is a process of oxidation of iron Fe^0 to Fe^{+2} . An additional capacitive peak observed in the range of higher frequencies (ok. 10^2 Hz) may be associated with the surface roughness. This is evidenced by value of the parameter $n = 0.6$, which is typical for processes that are under the diffusion control and which can be observed for example in the pores, discontinuities of the surface layer or in the surface roughness.

The results obtained by the potentiodynamic method agree with the impedance results. Nanobainitic structure produced in 67SiMnCr6-6-4 bearing steel does not affect significantly its corrosion resistance in comparison with steel after quenching and tempering with a similar hardness, irrespective of the corrosive environment (Fig. 6, Fig. 7, Table 4). The corrosion resistance in acidic environment changes very slightly for different heat treatments (Fig. 6). In case of neutral environment, the corrosion potential for nanostructured steel samples (A1) and quenched and tempered samples (QT1) with higher hardness is shifted toward positive values which indicates, that this materials start to corrode slightly later. However, the corrosion current densities are one order of magnitude higher as compared to the corresponding parameters measured for steels with lower hardness (A2, QT2), which indicates that

the corrosion rate at the initial stage is greater (Fig. 7). At the same time the corrosion resistance for individual materials is very similar, irrespective of the environment. No impact of different pH of a solution on the corrosion processes intensity was observed. This may indicate that the layer of iron oxides Fe_3O_4 formed at the surface of steel inhibit the electrochemical processes. The polarization curves obtained for all heat treated specimens are characteristic of uniform/general corrosion.

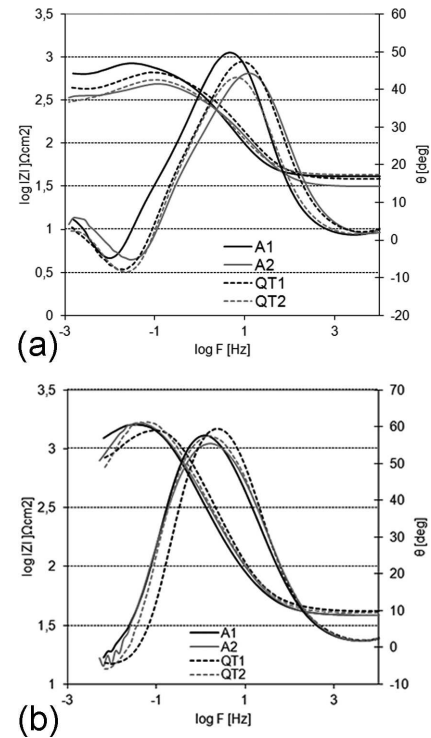


Fig. 5. Impedance spectra of 67SiMnCr6-6-4 bearing steel after various heat treatments in Na_2SO_4 acidic (a) and neutral (b) environment

TABLE 3

Characteristic electrochemical parameters of 67SiMnCr 6-6-4 bearing steel after various heat treatments in Na_2SO_4 acidic and neutral environment

treatment	parameter	pH4		pH7	
		Value1	Value2	Value1	Value2
A1	$R [\Omega cm^2]$	362.5	443	156	1540
	$Y_{CPE} [F/cm^2 * s^{n-1}]$	2.20E-03	4.40E-04	1.84E-03	6.00E-04
	n	0.92	0.83	0.63	0.92
A2	$R [\Omega cm^2]$	198.5	264	117.85	1755
	$C_{CPE} [F/cm^2] / Y_{CPE} [F/cm^2 * s^{n-1}]$	1.40E-03	3.20E-04	2.00E-03	5.60E-04
	n	1	0.8	0.63	0.92
QT1	$R [\Omega cm^2]$	247.5	395.5	338	1139
	$C_{CPE} [F/cm^2] / Y_{CPE} [F/cm^2 * s^{n-1}]$	1.50E-03	3.00E-04	1.04E-03	3.80E-04
	n	1	0.8	0.69	0.99
QT2	$R [\Omega cm^2]$	216.5	283.5	618	1214
	$C_{CPE} [F/cm^2] / Y_{CPE} [F/cm^2 * s^{n-1}]$	1.42E-03	4.00E-04	8.60E-03	6.80E-04
	n	1	0.81	0.69	1

$R [\Omega cm^2]$ – resistance, $Y_{CPE} [F/cm^2 * s^{n-1}] / C_{CPE} [F/cm^2]$ – capacity of CPE elements, n – parameter

Representative images of corrosion damage on the surface of 67SiMnCr6-6-4 bearing steel are shown in Fig. 8 and confirm the occurrence of general corrosion. In the case of steel after quenching and tempering treatment in lower temperature, regardless the corrosion environment, a number of pits were observed at the surface – probably caused by dissolution of secondary carbides or active nonmetallic inclusions.

TABLE 4

Characteristic electrochemical parameters of 67SiMnCr6-6-4 bearing steel after various heat treatments in Na₂SO₄ acidic and neutral environment

treatment	pH4		pH7	
	I _{kor} [μA/cm ²]	E _{kor} [mV]	I _{kor} [μA/cm ²]	E _{kor} [mV]
A1	10	-710	11	-635
A2	15	-710	1	-710
QT1	11	-710	11	-635
QT2	18	-720	2	-700

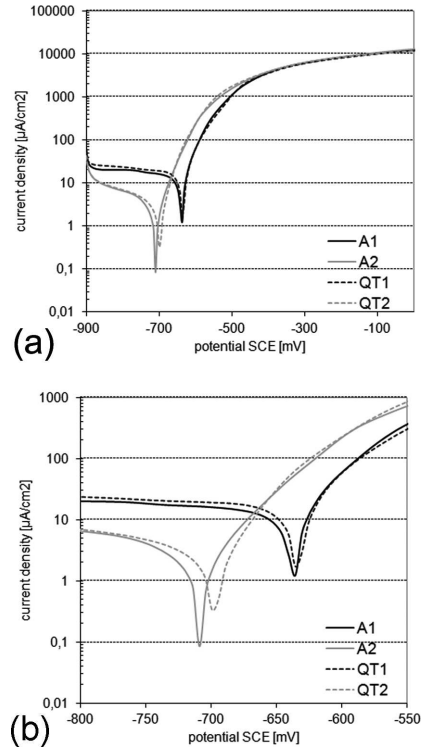


Fig. 7. Polarization curves obtained for 67SiMnCr6-6-4 bearing steel after various heat treatments in Na₂SO₄ neutral environment (b - magnification of the corrosion potential area)

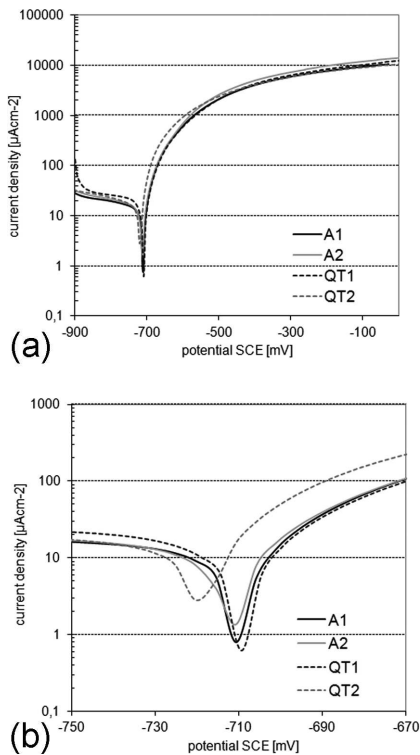


Fig. 6. Polarization curves obtained for 67SiMnCr6-6-4 bearing steel after various heat treatments in Na₂SO₄ acidic environment (b – magnification of the corrosion potential area)

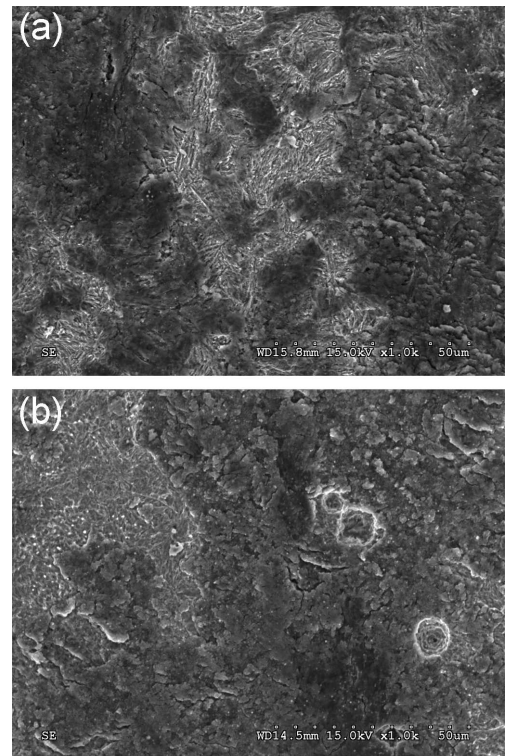


Fig. 8. Surface appearance of 67SiMnCr6-6-4 bearing steel after austempering (a) and quenching and tempering (b) after corrosion tests in Na₂SO₄ neutral environment

4. Summary

So called nanobainite, the nanocrystalline structure of the 67SiMnCr6-6-4 bearing steel, composed of bainitic ferrite plates separated by residual austenite layers, has been obtained by use of austempering heat treatment.

Electrochemical studies have shown that the corrosive resistance of the bearing steel with nanobainitic structure and high density of interphase α_B/γ_R boundaries is not worsened when compared to the tempered martensitic bearing steel with a similar hardness. The applied corrosion environment has no impact on the results.

The EIS method allowed revealing the presence of two phases of different corrosion rates: the retained austenite and ferritic bainite.

Acknowledgements

The results presented in this paper have been obtained within the project "Production of nanocrystalline steels using phase transformations" – NANOSTAL (contract no. POIG 01.01.02-14-100/09 with the Polish Ministry of Science and Higher Education). The project is co-financed by the European Union from the European Regional Development Fund within Operational Programme Innovative Economy 2007-2013.

REFERENCES

- [1] K.J. Kurzydłowski, M. Lewandowska (Eds), *Nanomateriały inżynierskie konstrukcyjne i funkcjonalne*. Wydawnictwo Naukowe PWN, 2010.
- [2] C. Garcia-Mateo, F.G. Caballero, H.K.D.H. Bhadeshia, *ISIJ International* **43**, 1238 (2003).
- [3] F.G. Caballero, H.K.D.H. Bhadeshia, K.J.A. Mawella, and D.G. Jones, P. Brown, *Materials Science and Technology* **18**, 279 (2002).
- [4] F.G. Caballero, H.K.D.H. Bhadeshia, *Current Opinion in Solid State and Materials Science* **8**, 251 (2004).
- [5] C. Garcia-Mateo, F.G. Caballero, *ISIJ International* **45**, 1736 (2005).
- [6] W. Burian, J. Marcisz, B. Garbarz, L. Starczewski, *Archives of Metallurgy and Materials* **59**, 1211 (2014).
- [7] H.K.D.H. Bhadeshia, *Ironmaking and Steelmaking* **32**, 405 (2005).
- [8] W.A. Świątnicki, K. Pobiedzińska, E. Skołek, A. Gołaszewski, Sz. Marciniak, Ł. Nadolny, J. Szawłowski, *Materials Engineering (Inżynieria Materiałowa)* **6**, 524 (2012).
- [9] J. Dworecka, K. Pobiedzińska, E. Jezierska, K. Roźniatowski, W. Świątnicki, *Materials Engineering (Inżynieria Materiałowa)* **2**, 109 (2014).
- [10] H. Garbacz, M. Pisarek, K.J. Kurzydłowski, *Biomolecular Engineering* **24**, 559 (2007).
- [11] El-Sayed M. Sherif, Asiful H. Seikh, *International Journal of Electrochemical Science* **7**, 7567 (2012).
- [12] E. Kus, Z. Lee, S. Nutt, F. Mansfeld, *Corrosion* **62**, 152 (2006).
- [13] G.R. Argade, S.K. Panigrahi, R.S. Mishra, *Corrosion Science* **58**, 145 (2012).
- [14] A. Dischino, J.M. Kenny, *Journal Of Materials Science Letters* **21**, 1631 (2002).
- [15] R. Mishra, R. Balasubramaniam, *Corrosion Science* **46**, 3019 (2004).
- [16] B. Hadzima, M. Janeček, Y. Estrin, H.S. Kim, *Materials Science and Engineering A* **462**, 243 (2007).
- [17] W. Zeiger, M. Schneider, D. Scharnweber, H. Worth, *NanoS-structured Materials* **6**, 1013 (1995).
- [18] K.D. Ralston, N. Birbilis, C.H.J. Davies, *Scripta Materialia* **63**, 1201 (2010).
- [19] E. Kus, Z. Lee, S. Nutt, F. Mansfeld, *Corrosion* **62**, 152 (2006).
- [20] A.T. Krawczynska, M. Gloc, K. Lublinska, *J Mater Sci.* **48**, 4517 (2013).
- [21] H.K.D.H. Bhadeshia, C. Garcia-Mateo, P. Brown, *Bainite steel and methods of manufacture thereof*, US 20110126946 A1, published 2 June 2011.